CdSe/ZnS (Core/Shell) Quantum Dots Multi-wallled Carbon Nanotubes (MWCNTs) on a Stainless Steel as a Photoanode in Solar Cells

Junthorn Udorn[1,3], Hayashi Sachio[1], Shengwen Hou[1], Chaoyang Li[1,2], Akimitsu Hatta[1,2] and Hiroshi Furuta[1,2]

[1]*Electronic and Photonic Systems Engineering, Kochi University of Technology, Tosayamada-cho, Kami, Kochi 782-0003, Japan*

[2]*Center for Nanotechnology, Research Institute, Kochi University of Technology, Tosayamada-cho, Kami, Kochi 782-0003, Japan*

[3]*Faculty of Engineering, Thai-Nichi Institute of Technology (TNI), 1771/1 Pattanakarn Rd. 37 Suanluang, Bangkok, 10250, Thailand*

Keywords: Multi-walled Carbon Nanotubes (MWCNTs), Quantum Dots (QDs), Quantum Dots Sensitized Solar Cells (QDSSCs), Power Conversion Efficiency (PCE).

Abstract: Multi-walled carbon nanotube (MWCNT) forests grown on a stainless steel substrate were used as a photoanode in CdSe/ZnS (core/shell) quantum dot (QD) sensitized solar cells (QDSSCs). QD-treated MWCNTs on the conductive metal stainless substrate showed a higher power conversion efficiency (PCE) of 0.014% than those grown on a doped silicon substrate with a PCE of 0.005% under AM 1.5 sunlight intensity (100 mW/cm^2). This higher efficiency can be attributed to the lower sheet resistance of 0.0045 Ω/sq for the metal substrate than the value of 259 Ω/sq for doped silicon. Additionally, the relationship between the reflectance of as-grown CNT and PCE is also examined. QDSSC fabricated from CNT of lower reflectance of 1.9 % at a height of 25 μm showed a better efficiency because the lower reflectance indicates the scattering of light repeatedly into deeper CNT forest resulting in higher absorption which indicates a higher surface area of CNTs to adsorb much amount of QDs on CNT forests, resulting in the higher PCE.

1 INTRODUCTION

The extraordinary mechanical, chemical, and electronic properties of carbon nanotubes (CNTs) make them outstanding materials for energy applications (Iijima 1991; Dong et al. 2011; Zhu et al. 2008). A major challenge in solar cell applications is the development of modified CNT structures for use as transparent electrodes (Cui et al. 2013). The modified CNT structure is expected to be a good material for use as a counter electrode or photo-anode (Cui et al. 2013) with semiconducting quantum dots (QDs) in order to harvest a broader range of light from the ultraviolet (UV) to the infrared (IR) (Hickey et al. 2000). We have reported a significant increase in optical total reflectance using a structural modification of CNT honeycombs (Udorn et al. 2016), which will increase the utility of CNT honeycomb structures in high-efficiency solar cells. QD-decorated CNTs exhibit efficient charge transfer from photo-excited QDs to the CNTs (Haremza et al. 2002). QD sensitized solar cells (QDSSCs) have attracted considerable interest from researchers because their power conversion efficiency (PCE) may exceed the Shockley and Queisser limits (Watanabe et al. 2011; Miller et al. 2012). In particular, QDs can harvest a broad range of optical wavelengths by multiple exciton generation (MEG), thus improving the photovoltaic efficiency (Péchy et al. 2001; Barve et al. 2012; Mar et al. 2011). Optical absorption by QDs fabricated from materials such as CdS (Yu et al. 2012), CdSe (Tian et al. 2013), and CdSe/ZnS (Baek et al. 2014) is intrinsically tunable from the UV to the near-IR due to the particle-size dependence of the bandgap. A major advantage of QDs as light sensitizers compared with conventional dyes is that electron recombination is suppressed, thereby improving the efficiency of QDSSCs (Hoke et al. 2012; Li et al.

Udorn J., Sachio H., Hou S., Li C., Hatta A. and Furuta H.
CdSe/ZnS (Core/Shell) Quantum Dots Multi-wallled Carbon Nanotubes (MWCNTs) on a Stainless Steel as a Photoanode in Solar Cells.
DOI: 10.5220/0006103801580163
In *Proceedings of the 5th International Conference on Photonics, Optics and Laser Technology (PHOTOPTICS 2017)*, pages 158-163
ISBN: 978-989-758-223-3

2012; Beard 2011). One dimensional (1D) wires, of e.g., TiO2 (Zarazúa et al. 2011; Guijarro et al. 2009), ZnO (Li et al. 2013; Zhang et al. 2009), and Si (Takahashi 2011; Jeyakumar et al. 2013) have been extensively used for electron transfer from QDs to electrodes. In particular, CNTs have arisen as a superior candidate 1D wire electrode material for QDSSC (Dong et al. 2011; Malara et al. 2011; Peng et al. 2011) because of their large surface area, high conductivity, high aspect ratio, and chemical stability. Due to their excellent electrical and thermal conductivity, flexible metal substrates can reduce both the sheet resistance and production cost of solar cells (Kang et al. 2006; Miettunen et al. 2008; Ma et al. 2004). To the best of our knowledge, there are no reports of QDSSCs in which QD-treated CNT forest photoanodes are fabricated on a metal substrate.

In this study, CNT forests grown on stainless steel serving as a photoanode for CdSe/ZnS core/shell QDSSCs are investigated as a means of improving photovoltaic efficiency. The efficiency was compared for samples of QDSSCs on a metal stainless steel substrate, QDSSCs on a doped silicon substrate, and QDSSCs with a photoanode of randomly oriented CNT (buckypaper) films on a metal stainless steel substrate. The relationship between the optical total reflectance of as-grown CNTs and the PCE was investigated.

2 MATERIAL AND METHODS

Vertically aligned multi-walled carbon nanotube (MWCNT) forests with tube diameters of 30–65 nm and heights of ~15 μm were prepared by a catalytic thermal chemical vapour deposition (CVD) method with an annealing time of 2.5 min in a hydrogen flow of 65 sccm at 28 Pa and 730°C, followed by CNT synthesis at 730°C with a carbon source gas of acetylene (C2H2) gas at 54 Pa for 10 min on Fe/Al (5/50 nm in thickness) bi-layered catalyst films on a sheet of stainless steel SUS304 (68% iron, 19% chromium, 10% manganese, 1% silicon, and 2% other compounds). The Fe/Al catalyst films on the stainless steel sheet were deposited by magnetron sputtering under an argon flow of 10 sccm, a pressure of 0.8 Pa, and a discharge current of 40 mA for 21 min for Al and 2.5 min for Fe. CNT buckypaper films were prepared by dipping vertically aligned CNTs grown on the stainless steel sheet into a methanol solution for 5 min, and then drying them in air at room temperature. The morphologies and heights of the as-grown CNT forests and modified CNT structures were characterized using field-emission scanning electron microscopy (FE-SEM; JEOL JSM-5310). The total reflectance in the UV–vis region was measured using a spectrophotometer (HITACHI U-3900). Solar cells were fabricated from as-grown CNT forests and CNT buckypaper films as photoanodes, treated with CdSe/ZnS (core/shell) quantum dots in toluene solutions as a sensitizer with a particle size of 3.4 nm (LumidotTM, Aldrich). Indium tin oxide (ITO) glass with a sheet resistance of ~15 Ω/sq was used as a counter electrode, and the 0.1-μm2 active area between the two electrodes was filled with an iodide electrolyte solution ($I1^-/I3^-$). The J–V characteristics of the cells were recorded with a computer-controlled digital source meter (Keithley Model 2400) by applying an external potential bias to the cell under AM 1.5 sunlight intensity (100 mW/cm^2). All measurement was carried out at the room temperature.

3 RESULTS AND DISCUSSIONS

Figures 1(a), (b), (c) display a top-view of FE-SEM micrographs of as-grown on a silicon substrate, the stainless steel substrate, and CNT buckypaper films on the stainless steel substrate, respectively. Inserted images of Fig.1(a), (b) and (c) show a cross-sectional image of as-grown on silicon substrates, on the stainless steel, and CNT buckypaper films, respectively. As can be seen in Figs. (a) and (b), the as-grown CNTs on the stainless steel shows an inconsistent height where as-grown CNTs on the silicon substrate shows a higher density and a consistent height. Meanwhile, CNT buckypaper films which were simply prepared by dipping vertically-aligned CNTs into a methanol solution for 5 min show a highly-packed randomly oriented CNTs as shown in an inset of Fig. 1(c). After QDs treatment, the self-assembly patterns can be formed, an inset of Fig. (b') shows a highly-magnified image of highly-packed CNTs where honeycomb-like patterns are formed on a silicon substrate as shown in Fig. 1(a').

The performance of the different substrates, patterns, and different heights is analysed by a sheet resistance, a series resistance, optical total reflectance, and power conversion efficiencies (PCE) as shown in Table 1. As-grown CNTs with a height of 25 μm on a stainless steel substrate with a sheet resistance of 0.0045 Ω/sq and an optical total reflectance of 1.9% at 560 m exhibit the highest PCE of 0.014%. Meanwhile, as-grown CNTs on a

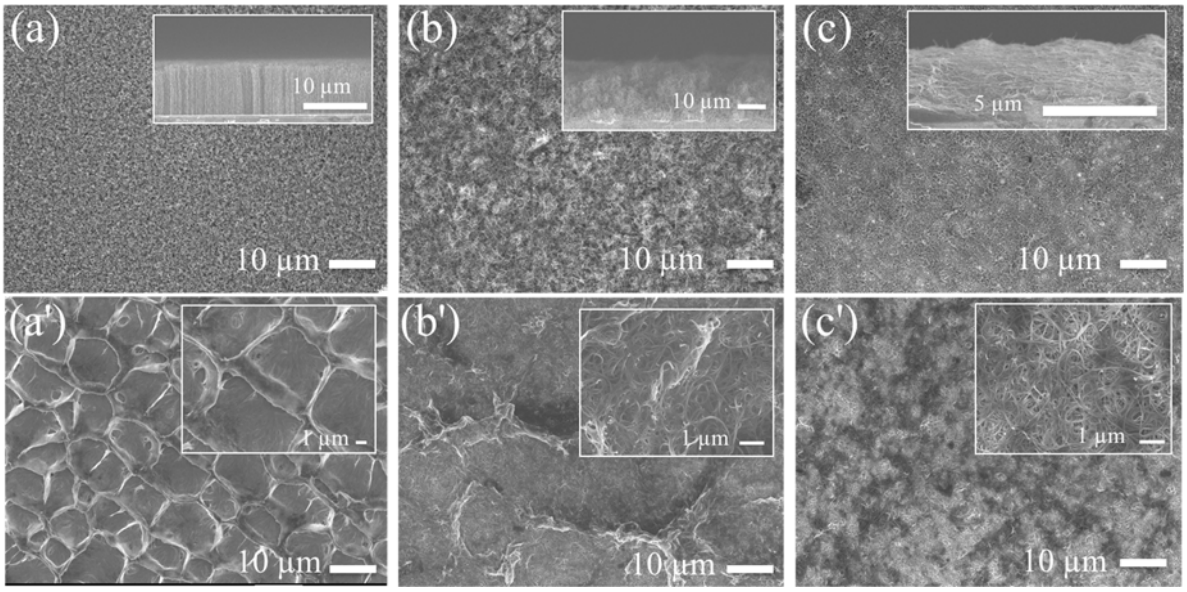

Figure 1: Top-view FE-SEM images of (a) as-grown CNTs on silicon substrate, (b) as-grown CNTs on stainless steel substrate, (c) CNT buckypaper films on stainless steel substrate. The insets show cross-sectional images. CdSe/ZnS QDs-treated on (a') as-grown CNTs on silicon substrate, (b') as-grown CNTs on stainless steel substrate, (c') CNT buckpaper films on stainless steel substrate. The insets show high-magnification images.

Table 1: Properties of QD-treated CNTs on a silicon substrate, and CNT buckypaper films on the stainless steel substrate, and QDs-treated CNTs on the stainless steel with various heights.

	Sheet resistance (Ω/sq)	**Series resistance (Ω/sq)**	**Total reflectance at 560 nm (without QDs)**	**J_{SC} (mA/cm^2)**	**V_{OC} (V)**	**FF**	**η (PCE)**
QD-treated CNTs on silicon substrate	259	33K	0.98%	0.067	0.21	38.6%	0.005%
QD-treated CNT buckypaper films on stainless steel	0.0046	14 K	4.3%	0.068	0.32	42.9%	0.009%
QD-treated 17-μm CNTs on stainless steel	0.0047	13K	4.1%	0.050	0.38	56.7%	0.011%
QD-treated 25-μm CNTs on stainless steel	0.0045	13K	1.9%	0.057	0.45	52.2%	0.014%
QD-treated 33-μm CNTs on stainless steel	0.0043	14K	2.2%	0.049	0.40	65.6%	0.013%
QD-treated 41-μm CNTs on stainless steel	0.0043	13K	2.2%	0.056	0.39	54.4%	0.012%

silicon substrate with a higher sheet resistance of 259 Ω/sq exhibit a PCE of 0.005%. The 2.8 times higher PCE for the former sample can be attributed to the higher conductance of the substrate. The PCE for QD-treated CNTs on the stainless steel substrate is 1.6 times higher than that for CNT buckypaper films on the same metal stainless steel substrate, which can be attributed to the higher number of QDs adsorbed on the surface of the CNTs. QD-treated CNTs on the stainless steel substrate had heights of 17, 25, 33 and 41 μm, and the PCE was the highest, at 0.014%, for a height of 25 μm. For the taller CNTs, the lower PCE could be explained by the fact that the electron transport path was longer than the electron diffusion length, leading to increased recombination of electrons and holes (Wei et al. 2014), and hence a lower efficiency.

Figure 2(a) shows the total reflectance of as-grown CNTs on a silicon substrate, a CNT buckypaper film on a stainless steel substrate, and as-grown CNTs of various heights on a stainless steel substrate. For as-grown CNTs on the stainless

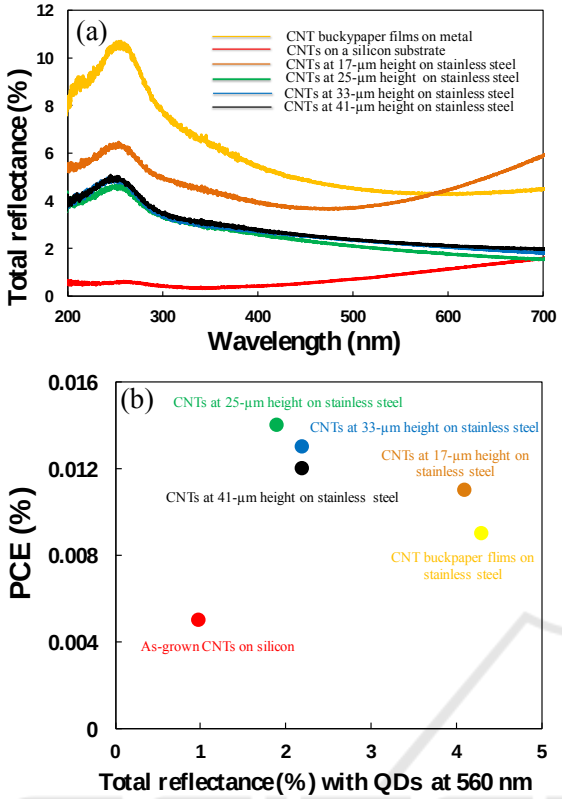

Figure 2: (a) Optical total reflectance of as-grown CNTs on a silicon substrate (red), CNT buckypaper films on the stainless steel substrate (yellow), as-grown CNTs on the stainless steel substrate in various heights, (b) PCE vs. total reflectance.

steel before QD treatment, the strong reflection at wavelengths shorter than 380 nm can be assigned to Rayleigh scattering, which provides a higher reflectance at shorter wavelength (Yu & and Louis Brus 2001). The bandgap of CdSe (E_g = 2.21 eV) is corresponded to 561 nm which is expected as an absorption edge of QDs. The CNT buckypaper films (black line) exhibit a higher total reflectance of more than 5% at 560 nm due to the highly packed CNTs serving as glassy carbon to strongly reflect light (Shabaneh et al. 2014). As-grown CNTs on a silicon substrate (grey line) exhibit the lowest total reflectance of less than 2%, which can be attributed to the higher density of CNT forests. The CNT forest with a height of 25 μm has a lower total reflectance of 1.9% at a wavelength of 560 nm. This can be explained by multiple scattering of the incident light into the bottom of the CNT forest, so-called blackbody absorption (Mizuno et al. 2009). Figure 2(b) shows the relationship between the total reflectance and the PCE, which indicates that the lower total reflectance of the as-grown CNTs on the stainless steel gives a higher solar cell efficiency after QDSSC fabrication. Significantly, the PCE for QDSSCs with CNTs with heights of 25 μm on a stainless steel substrate, with the total reflectance of 1.9% (green symbols), has a maximum value of 0.014%. Also, as can be seen in Fig. 2(b), the lower total reflectance of 25 and 33 μm exhibits the better PCE. The lower total reflectance due to efficient absorption of light in CNTs leads to higher solar cell efficiency. The low total reflectance of CNT forests, by the mechanism of the repeated reflection of incident light into the CNT bottom region, indicates a higher CNT surface area, which is expected to adsorb a larger number of QDs, resulting in a higher PCE.

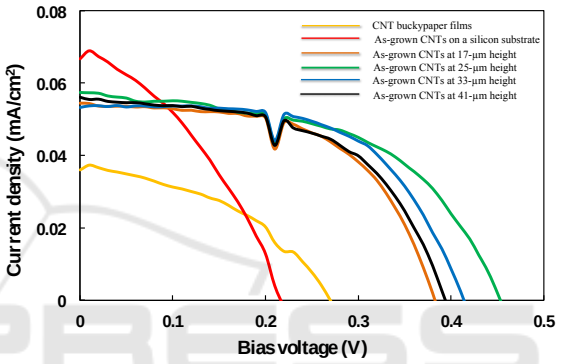

Figure 3: J–V curves of photovoltaic QDSSCs cells of QD-treated CNTs on silicon substrate, CNT buckypaper films on stainless steel substrate, QDs-treated CNTs with various heights on stainless steel substrates.

Figure 3 presents J–V curves for QDSSC cells of QD-treated CNTs on a silicon substrate, QD-treated CNT buckypaper films on a stainless steel substrate, and QD-treated CNTs with various heights on a stainless steel substrate. The PCE (η) was calculated using the equation $\eta = (FF \times J_{SC} \times V_{OC}) / P_{input}$, where FF is the fill factor and Pinput is the power density of the incident light. It can be seen that QD-treated CNTs with a height of 25-μm exhibit significantly better photovoltaic performance in terms of the current density (JSC) and the open-circuit voltage (VOC). Compared to those on the low-conductivity silicon substrate, as-grown CNTs after QD treatment on the stainless steel substrate also exhibit an improved open-circuit voltage of 0.21 to 0.45 volts (see Table 1). This is evidence that the low resistivity of the conductive substrate gives an increased open-circuit voltage, leading to improved solar cell efficiency. The QD-treated CNTs with heights of 25 μm exhibit a higher VOC of 0.45 volts and also slightly improves the VOC

from 0.32 to 0.45 volts as compared with CNT buckypaper films. In addition, the energy barrier at the QDSSC/CNT interface can suppress interfacial recombination, leading to an increased VOC, which is expected for CNT forests directly grown on metal substrates. The increase in the PCE is an indication of improved charge collection and transport due to introducing the CNTs forest directly grown on the metal substrate at a significant specific height as an electrode scaffold in the photoanode.

4 CONCLUSIONS

This study reported the first QDSSCs with photoanodes of MWCNTs on a metal substrate, and found that the PCE for such QDSSCs on stainless steel substrates was three times higher than those on a low-resistive (0.15 Ω·cm), doped silicon substrate. A QD-treated MWCNT forest on a metal substrate was found to have a resistance of 0.0045 Ω/sq and exhibited a higher PCE of 0.014%, whereas QD-treated MWCNTs on a doped silicon substrate had a resistance of 259 Ω/sq and a lower efficiency of 0.005%. This difference could be attributed to the fact that the very low sheet resistivity of a metal substrate gives a higher electrical conductance leading to a higher cell efficiency. The relationship between the total reflectance of CNT forests and the PCE was investigated. It was shown that the lower total reflectance QD-treated CNT forest of 25-μm height achieved a higher PCE of 0.014%, likely due to the higher light absorption in the QDs. Although the efficiency is currently low compared with that of high-performance DSSCs or QDSSCs, the successful incorporation of QDs with a CNT forest on a conductive substrate as a photoanode for solar cells has been demonstrated for the first time.

ACKNOWLEDGEMENTS

This work was supported by JSPS KAKENHI Grant (No.24560050) and also by a grant from Japanese Government (MEXT) Scholarship (No.132308).

REFERENCES

Baek, S.-W. et al., 2014. Effect of Core Quantum-dots Size on Power-conversion-efficiency for Silicon Solar-cells Implementing Energy-down-shift using CdSe/ZnS Core/Shell Quantum Dots. *Nanoscale*, 6, pp.12524-12531. Available at: http://pubs.rsc.org/en/Content/ArticleLanding/2014/NR/C4NR02472A [Accessed August 22, 2014].

Barve, A. V et al., 2012. Effects of contact space charge on the performance of quantum intersubband photodetectors. *Applied Physics Letters*, 100(19), p.191107.Available at: http://scitation.aip.org/content/aip/journal/apl/100/19/10.1063/1.4712601.

Beard, M.C., 2011. Multiple exciton generation in semiconductor quantum dots. *Journal of Physical Chemistry Letters*, 2(11), pp.1282–1288.

Cui, K. et al., 2013. Self-assembled microhoneycomb network of single-walled carbon nanotubes for solar cells. *Journal of Physical Chemistry Letters*, 4(15), pp.2571–2576. Available at: http://dx.doi.org/10.1021/jz401242a.

Dong, P. et al., 2011. Vertically aligned single-walled carbon nanotubes as low-cost and high electrocatalytic counter electrode for dye-sensitized solar cells. *ACS applied materials & interfaces*, 3(8), pp.3157–61. Available at: http://www.ncbi.nlm.nih.gov/pubmed/21770421.

Guijarro, N. et al., 2009. CdSe quantum dot-sensitized TiO2 electrodes: Effect of quantum dot coverage and mode of attachment. *Journal of Physical Chemistry C*, 113(10), pp.4208–4214.

Haremza, J.M. et al., 2002. Attachment of Single CdSe Nanocrystals to Individual Single-Walled Carbon Nanotubes. *Nano Letters*, 2(11), pp.1253–1258. Available at: http://pubs.acs.org/doi/abs/10.1021/nl025799m.

Hickey, S., Riley, D. & Tull, E., 2000. Photoelectrochemical studies of CdS nanoparticle modified electrodes: Absorption and photocurrent investigations. *The Journal of Physical Chemistry B*, 104(32), pp.7623–7626. Available at: http://pubs.acs.org/doi/abs/10.1021/jp993858n [Accessed June 26, 2014].

Hoke, E.T. et al., 2012. The role of electron affi nity in determining whether fullerenes catalyze or inhibit photooxidation of polymers for solar cells. *Advanced Energy Materials*, 2(11), pp.1351–1357.

Iijima, S., 1991. Helical microtubules of graphitic carbon. *Nature*, 354(6348), pp.56–58. Available at: http://www.nature.com/doifinder/10.1038/3540560 [Accessed July 10, 2014].

Jeyakumar, R., Maiti, T.K. & Verma, A., 2013. Influence of emitter bandgap on interdigitated point contact back heterojunction (a-Si:H/c-Si) solar cell performance. *Solar Energy Materials and Solar Cells*, 109, pp.199–203.

Kang, M.G. et al., 2006. A 4.2% efficient flexible dye-sensitized TiO_2 solar cells using stainless steel substrate. *SOLAR ENERGY MATERIALS AND SOLAR CELLS*, 90(5), pp.574–581.

Li, C. et al., 2013. Photovoltaic property of a vertically aligned carbon nanotube hexagonal network assembled with CdS quantum dots. *ACS applied materials & interfaces*, 5(15), pp.7400–4. Available at: http://www.ncbi.nlm.nih.gov/pubmed/23844806.

Li, Y. et al., 2012. Annealing Effect on Photovoltaic Performance of CdSe Quantum-Dots-Sensitized TiO_2 Nanorod Solar Cells, 2012, pp.1-6.

Ma, T.L. et al., 2004. Properties of several types of novel counter electrodes for dye-sensitized solar cells. *Journal of Electroanalytical Chemistry*, 574(1), pp.77–83. Available at: <Go to ISI>:// 000225310800010.

Malara, F. et al., 2011. Flexible carbon nanotube-based composite plates as efficient monolithic counter electrodes for dye solar cells. *ACS Applied Materials and Interfaces*, 3(9), pp.3625–3632.

Mar, J.D. et al., 2011. Voltage-controlled electron tunneling from a single self-assembled quantum dot embedded in a two-dimensional-electron-gas-based photovoltaic cell. *Journal of Applied Physics*, 110(5),p.053110. Available at: http://scitation.aip.org/content/aip/journal/jap/110/5/10.1063/1.3633216.

Miettunen, K. et al., 2008. Initial Performance of Dye Solar Cells on Stainless Steel Substrates. *Journal of Physical Chemistry C*, 112(10), pp.4011–4017. Available at: http://pubs.acs.org/cgi-bin/doilookup/?10.1021/jp7112957.

Miller, O.D., Yablonovitch, E. & Kurtz, S.R., 2012. Strong internal and external luminescence as solar cells approach the Shockley-Queisser limit. *IEEE Journal of Photovoltaics*, 2(3), pp.303–311.

Mizuno, K. et al., 2009. A black body absorber from vertically aligned single-walled carbon nanotubes. *Proceedings of the National Academy of Sciences of the United States of America*, 106(15), pp.6044–6047.

Péchy, P. et al., 2001. Engineering of Efficient Panchromatic Sensitizers for Nanocrystalline TiO2-Based Solar Cells. *Journal of the American Chemical Society*, 123(8), pp.1613–1624. Available at: http://pubs.acs.org/doi/abs/10.1021/ja003299u.

Peng, T. et al., 2011. Hydrothermal Preparation of Multiwalled Carbon Nanotubes (MWCNTs)/CdS Nanocomposite and Its Efficient Photocatalytic Hydrogen Production under Visible Light Irradiation. *Energy & Fuels*, 25(5), pp.2203–2210. Available at: http://dx.doi.org/10.1021/ef200369z.

Shabaneh, A.A. et al., 2014. Reflectance Response of Optical Fiber Coated With Carbon Nanotubes for Aqueous Ethanol Sensing. *IEEE Photonics Journal*, 6(6), p.6802910.

Takahashi, T., 2011. Photoassisted Kelvin probe force microscopy on multicrystalline Si solar cell materials. In *Japanese Journal of Applied Physics*, 50, p.08LA05.

Tian, J. et al., 2013. ZnO/TiO2 nanocable structured photoelectrodes for CdS/CdSe quantum dot co-sensitized solar cells. *Nanoscale*, 5(3), pp.936–943. Available at: http://dx.doi.org/10.1039/C2NR32663A.

Udorn, J., Hatta, A. & Furuta, H., 2016. Carbon Nanotube (CNT) Honeycomb Cell Area-Dependent Optical Reflectance. *Nanomaterials*, 6(11), p.202. Available at: http://www.mdpi.com/2079-4991/6/11/202.

Watanabe, K. et al., 2011. Si/Si 1-xGe x nanopillar superlattice solar cell: A novel nanostructured solar cell for overcoming the Shockley-Queisser limit. In *Technical Digest - International Electron Devices Meeting, IEDM*, pp. pp: 36.4.1-36.4.4. Available at: http://ieeexplore.ieee.org/document/6131685/

Wei, J. et al., 2014. Modification of carbon nanotubes with 4-mercaptobenzoic acid-doped polyaniline for quantum dot sensitized solar cells. *Journal of Materials Chemistry C*, 2, pp.4177–4185. Available at: http://xlink.rsc.org/?DOI=c4tc00021h.

Yu, K. et al., 2012. Controllable photoelectron transfer in CdSe nanocrystal-carbon nanotube hybrid structures. *Nanoscale*, 4(3), pp.742–746. Available at: http://dx.doi.org/10.1039/C2NR11577H.

Yu, Z. & and Louis Brus, 2001. Rayleigh and Raman Scattering from Individual Carbon Nanotube Bundles. *The Journal of Physical Chemistry B*, 105(6), pp.1123–1134. Available at: http://dx.doi.org/10.1021/jp003081u.

Zarazúa, I. et al., 2011. Photovoltaic conversion enhancement of CdSe quantum dot-sensitized TiO 2 decorated with Au nanoparticles and P3OT. *Journal of Physical Chemistry C*, 115(46), pp.23209–23220.

Zhang, Y. et al., 2009. Surface photovoltage characterization of a ZnO nanowire array/CdS quantum dot heterogeneous film and its application for photovoltaic devices. *Nanotechnology*, 20(15), p.155707. Available at: http://stacks.iop.org/0957-4484/20/i=15/a=155707.

Zhu, H.W. et al., 2008. Anthocyanin-sensitized solar cells using carbon nanotube films as counter electrodes. *Nanotechnology*, 19(46), p.5. Available at: <Go to ISI>://000260264000007.